sustainability

MDPI

Article

Utilization of Municipal Solid Waste Incineration Bottom Ash as Fine Aggregate of Cement Mortars

Byeong-Hun Woo [1], In-Kyu Jeon [2], Dong-Ho Yoo [1], Seong-Soo Kim [3], Jeong-Bae Lee [4] and Hong-Gi Kim [1,*]

[1] Civil and Environmental Engineering Department, Hanyang University, Jaesung Civil Engineering Building, 222 Wangsimni-ro, Seongdong Gu, Seoul 04763, Korea; dimon123@hanyang.ac.kr (B.-H.W.); dongho3461@naver.com (D.-H.Y.)
[2] Zachry Department of Civil & Environmental Engineering, Texas A&M University, College Station, TX 77843, USA; wjsdlsrb5474@tamu.edu
[3] Department of Civil Engineering, Daejin University, 1007 Hoguk-ro, Pocheon-si 11159, Korea; sskim@daejin.ac.kr
[4] GFC R&D Co., Ltd., 155 Hoguk-ro, Pocheon-si 11158, Korea; dlwjdqo@nate.com
* Correspondence: dmkg1404@hanyang.ac.kr; Tel.: +82-222-204-323

Abstract: Incineration bottom ash is generated by the incineration of solid waste. Household solid waste is increasing every year and so is incineration bottom ash. This is a problem to treat the incineration bottom ash because the ash has many toxic components. Cement composites can solve this problem and there are many studies for using the bottom ash as fine aggregate. To evaluate the usage of incineration bottom ash, compressive strength, mercury intrusion porosimetry, scanning electron microscopy-backscatter electron, X-ray diffraction, and toxicity characteristic leaching processes were performed. When using incineration bottom ash up to 20% of substitution, the compressive strength in all cases was increased. This study showed how the filler effect appeared well in the cement composites through the scanning electron microscopy-backscatter electron, and mercury intrusion porosimetry. X-ray diffraction indicated the possibility of an alkali-silica reaction of the aggregate with the components of incineration bottom ash. This problem is an obstacle to applying the incineration bottom ash as a fine aggregate. In addition, the toxicity characteristic leaching process was shown to be under the threshold of the Korean standard, however, this should nuanced by the consideration of amorphity. Comprehensively, incineration bottom ash could be used as a fine aggregate of up to 20% of substitution. However, the pre-treatment would need to eliminate or reduce alkali reactive components and heavy metals.

Keywords: incineration bottom ash; substitution; fine aggregate; heavy metal; leaching

Citation: Woo, B.-H.; Jeon, I.-K.; Yoo, D.-H.; Kim, S.-S.; Lee, J.-B.; Kim, H.-G. Utilization of Municipal Solid Waste Incineration Bottom Ash as Fine Aggregate of Cement Mortars. *Sustainability* **2021**, *13*, 8832. https://doi.org/10.3390/su13168832

Academic Editor: Jorge de Brito

Received: 12 July 2021
Accepted: 4 August 2021
Published: 6 August 2021

1. Introduction

It has been recognized for decades that the huge amount of waste produced by modern society causes a critical environmental impact [1]. Thus, the importance of recycling and the reuse of solid waste in the industrial field is increasing and several studies has been done on different ways this can achieved [2,3]. The municipal solid waste (MSW) incineration method, which has the advantage of reducing the mass and volume of the initial waste, is increasingly used as a waste treatment method in most developed countries [4]. From the incineration work, many types of ash are generated. In particular, MSW incineration bottom ash (IBA) accounts for the largest portion (about 80%) of the incineration process and generally consists of minerals, glass, ceramics, metallics, and unburned organic matter [5,6]. The chemical composition of the IBA is influenced by raw waste materials, so there may be some regional or seasonal differences.

Cabrera et al. [7] expected that incineration of MSW worldwide will increase due to increases in consumption and the limitations of landfills. Global MSW generation is expected to reach 2.2 billion tons by 2025 [8]. Seo [9] found that South Korea produced

18.6 million tons of MSW in 2009 and that production is due to increase in the future. Although the incineration method is an effective way to reduce the mass and volume of MSW by about 80% to 90%, it still generates a large amount of IBA and air pollution control materials [10]. The IBA, which accounts for 80% of the total residue is mainly handled by landfills, causing many problems in processing due to the lack of landfill sites. Therefore, a number of studies are being conducted actively to recycle IBA by its use as an industrial or construction material [11–13]. One of the main methods to recycle IBA is its use as the aggregate to produce road materials and cement composite. Le et al. [14] used IBA as an aggregate in road construction such as a road base, embankment, and asphalt pavement. In addition, the researchers also found that IBA is a non-hazardous material and has enough geotechnical and mechanical properties to use for earthwork and road construction [14]. Tang et al. [15], Lynn et al. [16], and Siddique [17] studied using IBA as an aggregate to make concrete, and experimental results shows that mechanical and durability properties of concrete containing IBA reduced with an increased replacement ratio of IBA. However, the reduction ratio can be minimized by pretreatment of IBA, such as washing.

Previous research mainly studied the influence of IBA content on the mechanical and durability properties of cement composite with IBA as the substitute for natural aggregate. However, only a few studies have been conducted to minimize the reduction of mechanical properties through pretreatment like washing to use IBA as aggregate. Generally, it takes more than 3 months for the weathering process. In addition, pretreated IBA still showed a somewhat lower strength development and durability performance compared to natural aggregate. This study aims to assess the usability of IBA through the mechanical and microstructure properties of cement mortar. To apply the IBA as a fine aggregate, compared to natural aggregate, used cement mortar by adding a sieving process to the conventional pretreatment process in order to decrease the particle size of IBA.

Based on a review of current literature, it can be said that pretreated IBA can improve the mechanical and microstructure performance of cement composites. For this purpose, mortar specimens were prepared by replacing natural fine aggregate with various contents of pretreated IBA. Specimens were investigated using a compressive strength test, mercury intrusion porosimetry (MIP), scanning electron microscopy-backscatter electron mode (SEM-BSE), X-ray diffraction (XRD), and a toxicity characteristic leaching procedure (TCLP) test.

2. Experimental Program

2.1. Materials

In this study, ordinary Portland cement (OPC, Type I–12 MPa of compressive strength at 7 days only for paste) complying with ASTM C150 [18] was used for the binder material. Natural river sand with a maximum size of 5 mm, fineness modulus (F.M) of 2.7, and absorption of 1.05% was used as the fine aggregate [19]. Incineration bottom ash (IBA) was collected from a waste incineration plant located in Hongcheon (South Korea). Figure 1 shows the schematic diagram of the incineration process in the H waste incineration plant. The feed stream treated in this H incineration plant consists mainly of local household rubbish. About 2000 tons of IBA are produced as incineration residues at H plant annually and are mostly treated as landfills. The unprocessed IBA was brought to the laboratory and used as a substitute for natural fine aggregate after a treatment process. The chemical composition of IBA obtained from X-ray fluorescence (XRF) are presented in Table 1. Furthermore, Figure 2 represents the particle size distribution (Malvern Mastersizer 3000) of pretreated IBA and natural aggregate. Figure 3 shows the particle shape of IBA obtained via SEM analysis.

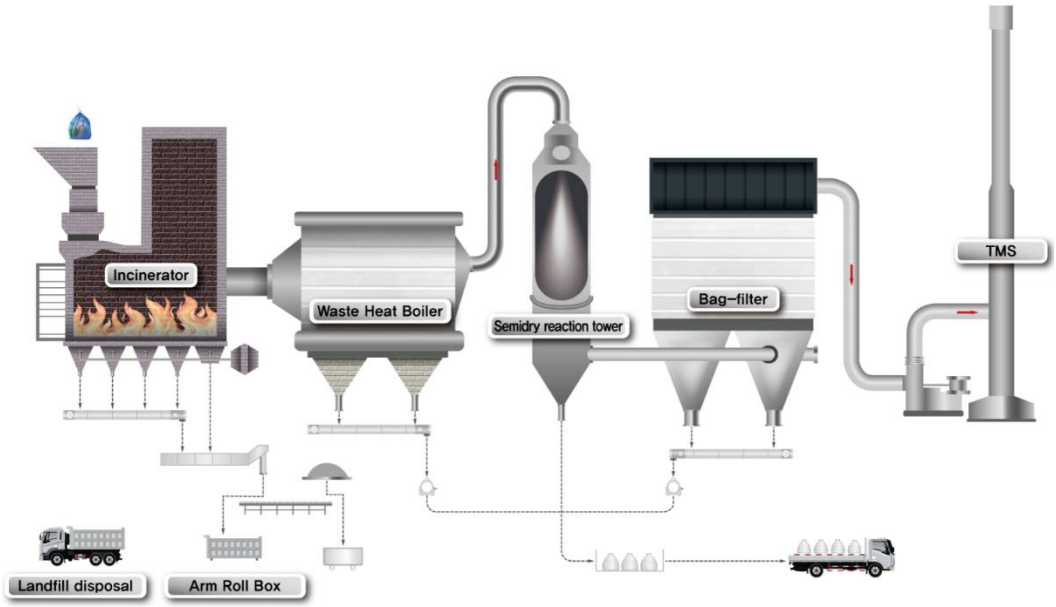

Figure 1. Schematic diagram of incineration process in H waste incineration plant.

Table 1. The chemical composition of IBA.

Composition	CaO	P_2O_5	Al_2O_3	SiO_2	Fe_2O_3	MgO	SO_3	TiO_2	Na_2O	Cl	K_2O	L.O.I
Weight occupancy (%)	43.97	12.01	10.3	8.98	7.79	4.96	3.02	2.12	1.95	1.83	0.99	1.24

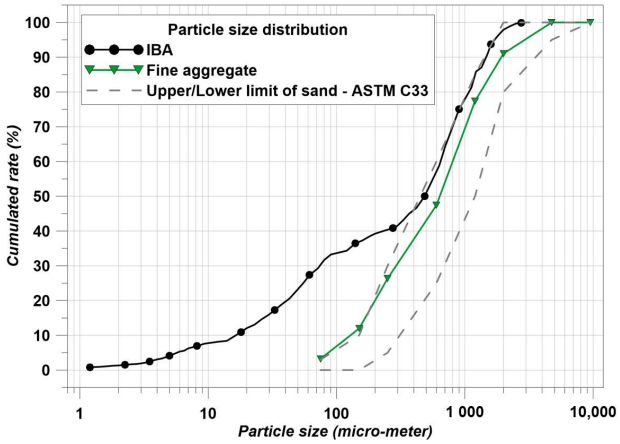

Figure 2. Particle size distributions of IBA and natural fine aggregate.

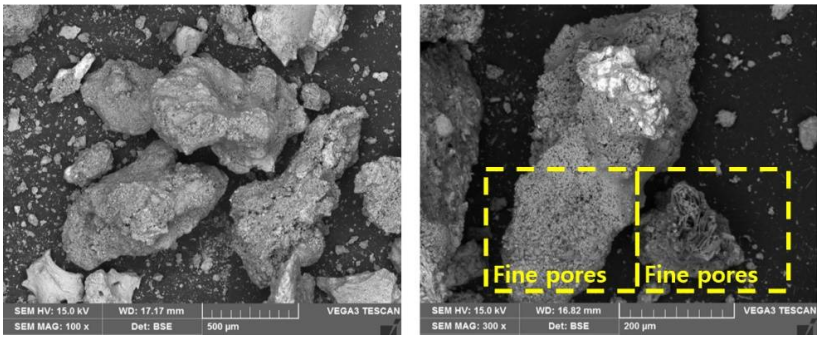

Figure 3. SEM image of IBA aggregate.

2.2. Preparation of Municipal Solid Waste Incineration Bottom Ash

In this study, in order to develop the aggregate quality and remove impurities, a washing and sieving procedure were used as a pretreatment method. Unlike previous literatures [20–22] where IBA was left in the natural environment for more than 3 months, the IBA used in this study was taken directly from the H waste incineration plant and the pretreatment process was carried out separately. The schematic diagram of the pretreatment process of the IBA is shown in Figure 4. First, untreated raw IBA was located on the No. 4 sieve and washed using flowing water to reduce clumps and remove impurities such as large scales of glass, ceramic debris, and metal residue. Second, washed IBA was placed in a dry oven for 4 h at 105 °C to evaporate the surface water in the IBA and to prevent the cohesion phenomenon. After the drying procedure, the IBA was classified by the No. 8 sieve to maximize the particle packing effect inside the cement matrix by keeping the small size of the aggregate.

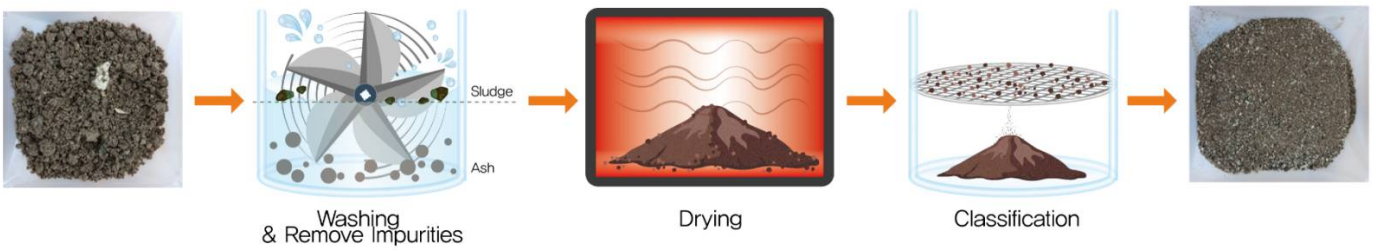

Figure 4. Schematic representation of the IBA preparation and pretreatment process.

2.3. Mix Proportions and Fabrication of Mortar Specimens

The mortar mixes used in this study were made with a constant water/binder ratio of 0.4 and a 1:2 ratio of binder to fine aggregate (natural river sand including replaced IBA). The mortar mixes used in this study were named IBA0, IBA5, IBA10, IBA15, and IBA20. For example, Mortar mix IBA0 was the control specimen without IBA aggregate. The mortar mixes IBA5, IBA10, IBA15, and IBA20 represent those containing 5%, 10%, 15%, and 20% of IBA aggregate as a natural sand replacement, respectively. The details of the mix design are indicated in Table 2. The mix constituents were dry mixed before the addition of water.

Table 2. Mixture design of specimens.

Composition	W/C (%)	Water (g)	Cement (g)	Fine Aggregate (g)	IBA (g)	Water Reducer (g)
IBA0	40	280	700	1400	0	7
IBA5				1330	70	
IBA10				1260	140	
IBA15				1190	210	
IBA20				1120	280	

Mortar cubes ($50 \times 50 \times 50$ mm^3) were prepared in accordance with ASTM C 109 [23], respectively. All mortar specimens were demolded after 24 h and kept in water at 23 ± 2 °C for curing until the desired duration was reached.

2.4. Methods

In this study, to investigate the effect of the IBA aggregate on the mechanical properties, compressive strength tests on the mortar specimens were conducted using a universal machine (Shimadzu, CCM-200A; Shimadzu Corporation, Kyoto, Japan) according to ASTM C 109 [23], after 3, 7, and 28 days of water curing. For each test, three replicates were measured, and the average value was recorded.

To identify the effect of IBA aggregate as a filler on the microstructure of cement composite, a porosity measurement test was performed using the MIP method [24]. For

the MIP, Micromeritics Autopore 9520 and a scanning electron microscope (accelerating voltage: 0.2–30 kV, probe current: 10×10^{-12} to 10×10^{-5} A, SEI resolution: 3.5 nm, and magnification: 10 times to 300,000 times) was used in this experiment. Equation (1) is to calculate the pore diameter [25].

$$\gamma = -2\delta\cos\theta/p \quad (1)$$

where γ is the radius of the pore (μm), δ is the surface tension of mercury (N/m): 0.484 N/m, θ is a contact angle between the specimen and mercury (degree): 130°, p is an input pressure of mercury (MPa): 206.84 MPa (30,000 psi). When the p is higher, a smaller pore diameter could be measured.

Samples for SEM-BSE analysis were carried after compressive strength test and immersed in alcohol to stop the hydration procedure and then dried in an oven at 60 °C, according to previous literature [26].

To analyze the presence of IBA and the hydration effect in the cement matrix, XRD (RINT D/max2500, 40 kV, 30 mA, scanning speed: 2°/min, wavelength: 1.54 Å) was conducted in this study.

The heavy metal content was analyzed using the TCLP test in accordance with the USEPA Method 1311 [27]. IBA mortar samples were crushed after the compressive strength test with 28 days curing to remove the large particles through 10 mm sieve. The TCLP test utilizes an acetic acid (pH 2.88) with a liquid to solid ratio of 20:1 and an extraction period of 18 h using a rotary tumbler at 30 ± 2 rpm. After extraction, the leachate was filtered through a 0.22 μm filter and stored in chamber at a temperature of 4 °C. The metal concentrations (Cr, Cd, Pb, and Zn) of leachate samples were measured in this study. Before measuring inductively coupled plasma mass spectrometry (ICP-MS, Perkin Elmar, NexION300), the authors measured the pH of the leachate solution and added a small amount of nitric acid until pH < 2 and conducted ICP-MS. Figure 5 presents the structure of ICP-MS.

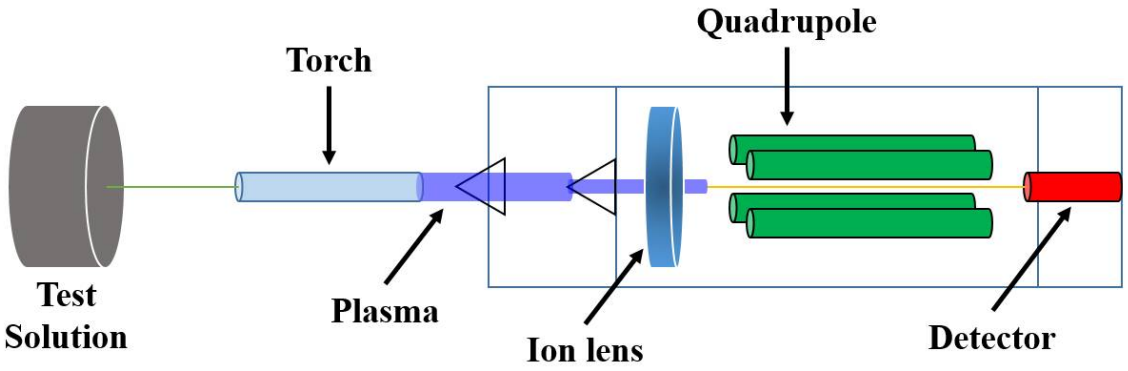

Figure 5. The structure of ICP-MS tester.

3. Results and Discussion

3.1. Compressive Strength Results

IBA was used as a fine aggregate, therefore the use of IBA affected the compressive strength. The results of compressive strength are indicated in Figure 6. The used natural sand had the range of particle size recommend by ASTM C33 [19]. However, studies on the filler effect of fine aggregates were considered many times, the importance of fine particles was increasingly emphasized [28–30]. According to Figure 2, IBA had a wider range of particle size than the natural sand. Therefore, IBA could create the filler effect due to the fine particle size [28]. The substituted IBA specimens showed an increase in compressive strength. This trend could be considered the filler effect [28–30].

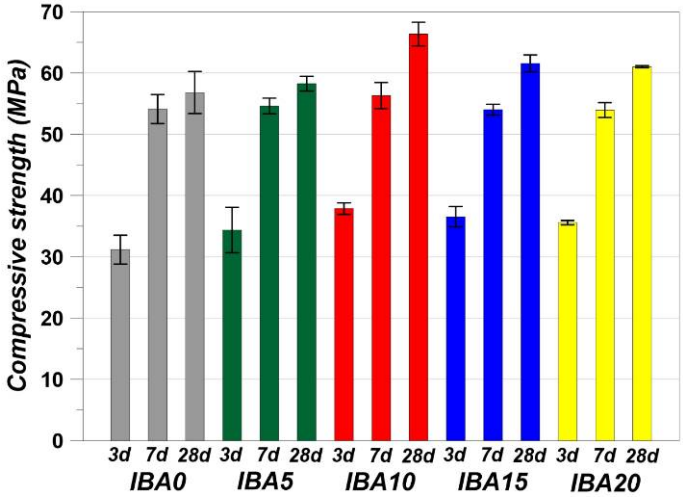

Figure 6. Compressive strength results.

According to Figure 6, IBA5 showed a small increase in compressive strength, but IBA10 showed a large increase in compressive strength. IBA20 showed an almost average strength of IBA5 and IBA10. The particle size of IBA and natural sand overlapped a substantial amount except for under 75 μm. The overlapping area compensates for the absence of natural sand by substituting it and the remaining particles under 75 μm have a filler effect. This is further elucidated in Figure 7. According to Figure 6, IBA0, IBA10, and IBA20 were chosen as key specimens due to the trend of the compressive strength. From Figure 7, it is possible to estimate that the fine particle content of IBA5, under 75 μm, is approximately 1.42% of the aggregate volume. An occupancy of 1.42% is not able to increase the compressive strength significantly. However, the particle distribution in Figure 7 is more homogeneous (details are in Chapter 3.2) than IBA0 due to particle compensation, which shows that IBA10 exhibits the highest compressive strength. In this context, IBA20 should have shown the highest compressive strength, but the strength of IBA20 decreased. This is because IBA is a lightweight aggregate [31]. The fine pores in IBA could be observed in Figure 3. Typically, the mechanical properties are decreased by using a lightweight aggregate [32]. Hence, IBA20 showed a reduction in the compressive strength despite the increase of fine particles under 75 μm.

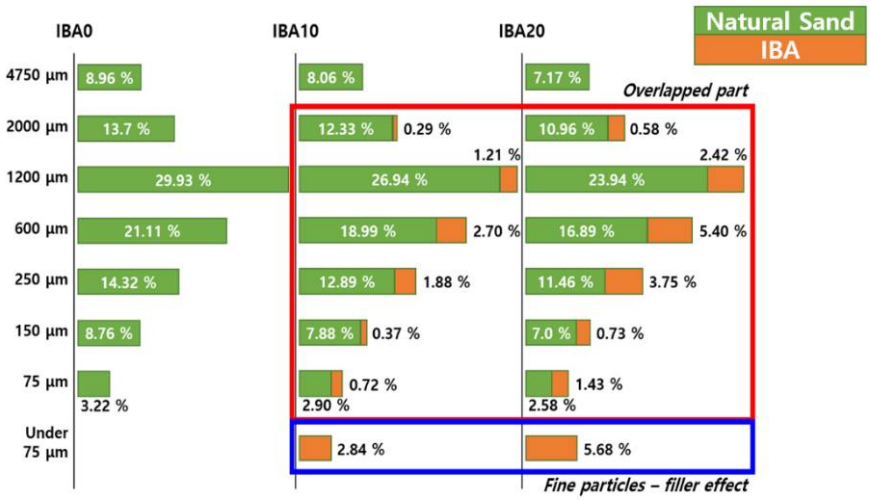

Figure 7. Size distribution of aggregates.

3.2. Mercury Intrusion Porosimetry Results

IBA10 and IBA20 were determined as the key specimens because the results of IBA5 and IBA15 are able to estimate using IBA10 and IBA20. MIP results are indicated in Figures 8 and 9. Figures 8 and 9 demonstrate the filler effect seen in Figure 7 and it can be confirmed that the pore volume is decreased with the increase of IBA. In addition, the particle compensation can be observed at a micro-scale to macro-scale (M-M scale, upper than 10,000 nanometers) from Figure 8. Compared to Figure 7, IBA0 and IBA10 showed almost the same pore distribution at the M-M scale, and this trend is the same as in Figure 7. The difference is that the porosity of more than 200,000 nanometers had been reduced, which can be evaluated as the porosity reduction effect brought by IBA. On the other hand, in the micro-scale to nano scale (M-N scale, lower than 10,000 nanometers), it is hard to evaluate the pore status in Figure 8. The reduction rate of pores can be confirmed more easily in Figure 9. At the M-N scale, IBA10 showed a smaller pore volume than IBA0, and this is further evidence of the filler effect. In the case of IBA20, although the compressive strength of IBA20 was relatively decreased compared to IBA10 [31,32], IBA20 showed a smaller pore volume than IBA10. This is because IBA20 was more significantly substituted for the fine aggregate compared to IBA10, therefore IBA20 had more fine particles compared to IBA10. This phenomenon has already demonstrated by many experimental studies [6,28–30] and was expected in our results.

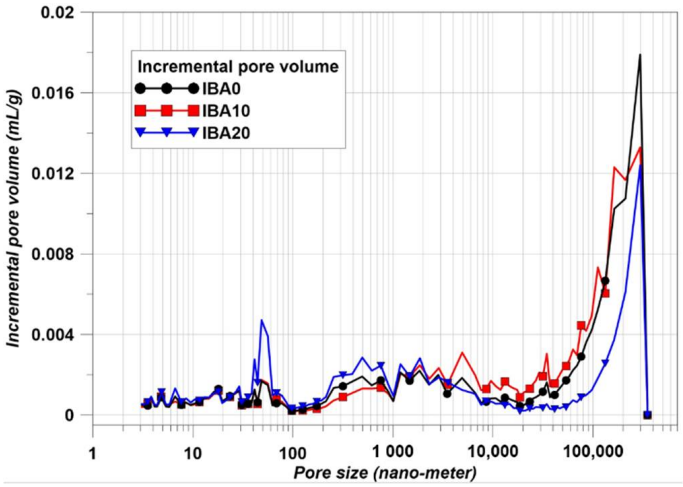

Figure 8. Incremental pore volume results.

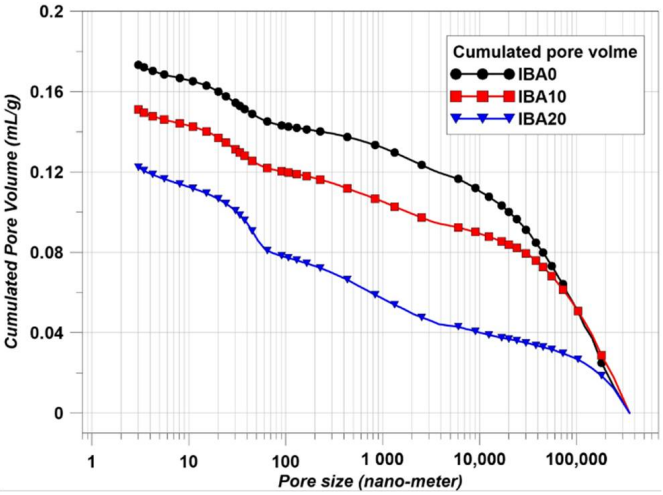

Figure 9. Cumulated pore volume.

3.3. SEM-BSE Image Analysis

Based on the results of MIP, IBA20 showed the least pore distribution. Therefore, it is possbible to compare IBA0 and IBA20 in this study. SEM-BSE image results are presented in Figure 10. The featured area indicates specific components. Area A is the fine aggregate (natural sand), area B is the pore, area C is the capillary pore, and area D is the IBA [33,34]. Natural sand and IBA can be easily distinguished in BSE images. Natural sand has a smooth section in Figure 10, however, IBA shows that there are many fine pores as also seen in Figure 3. Therefore, the strength reduction of IBA15 and IBA20 could be explained using Figure 10b [31,32].

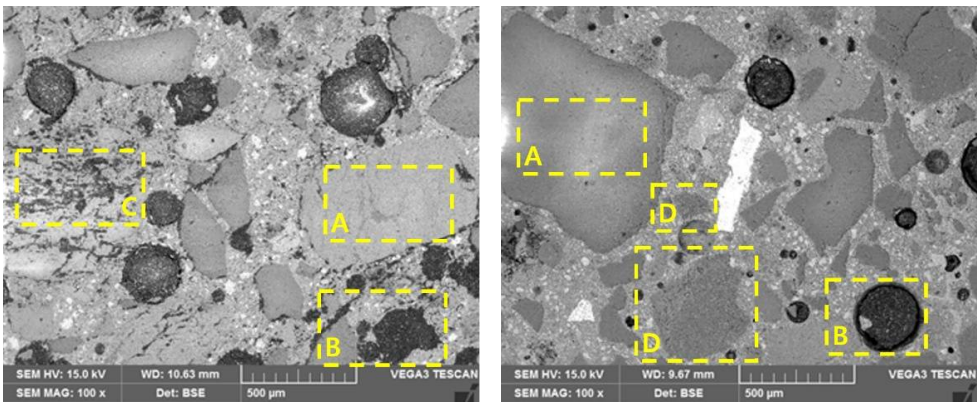

(**a**) IBA0 (**b**) IBA20

Figure 10. SEM-BSE images of IBA0 and IBA20.

The biggest difference between IBA0 and IBA20 is the pore distribution shown in Figure 10. In the case of IBA0, the capillary pores were observed. However, the capillary pores are rarely found in IBA20. In addition, the amount of part B in Figure 10 is clearly decreased in IBA20 compared to IBA0. This is the filler effect in line with the previous sections [28,30].

3.4. XRD Analysis

The XRD results are presented in Figure 11. The main elements such as portlandite and CSH were identified in the XRD results, and changes in intensity were also identified with curing ages. The existence of quartz means natural sand and the intensity of quartz did not change at all curing ages. However, there were peak changes in CSH and portlandite. From the results of XRD and Table 1, a critical factor was observed: the possibility of a alkali-silica reaction (ASR). According to Figure 11, IBA10 and IBA20 showed less content of portlandite than IBA0, and this suggests the possibility of an alkalinity reaction [35]. The alkalinity components could react with the component of Na_2O and K_2O as the main ingredient of ASR [35]. The high alkalinity cement includes the Na_2O of approximately 0.73 to 1.02% [35]. However, IBA contains 1.95% of Na_2O. This means IBA is a kind of reactive aggregate, therefore some treatments is needed to reduce Na_2O and K_2O when using the IBA as an aggregate. Except for this critical factor, the trends of the XRD results were the same in all specimens.

3.5. TCLP Results

The ICP-MS results are presented in Figure 12. According to Figure 12, a large amount of heavy metals were leached from the raw IBA, and IBA10 confirmed a significant decrease in leaching of all heavy metals except for Cd. On the other hand, naturally, IBA20 showed increased leaching of heavy metals due to the higher substitution rates compared with other specimens. In particular, leached Zn of IBA20 showed almost the same level as raw IBA.

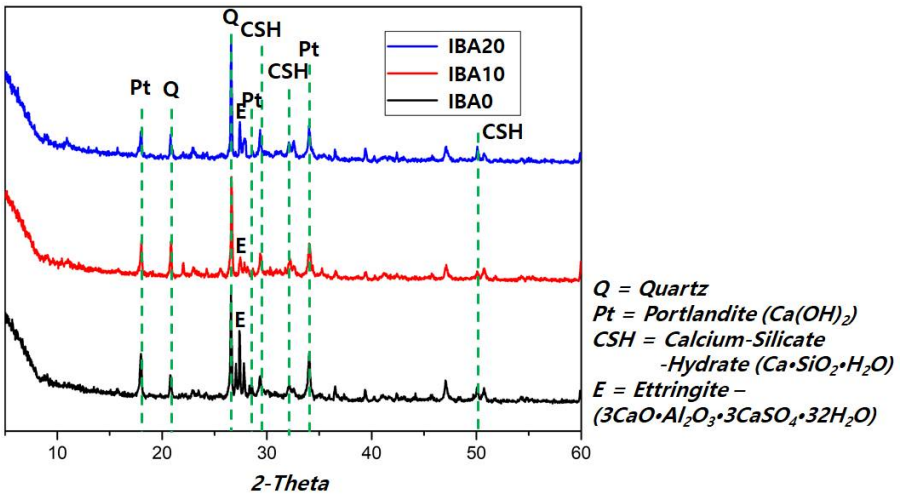

(**a**) XRD results after 3 days of curing ages

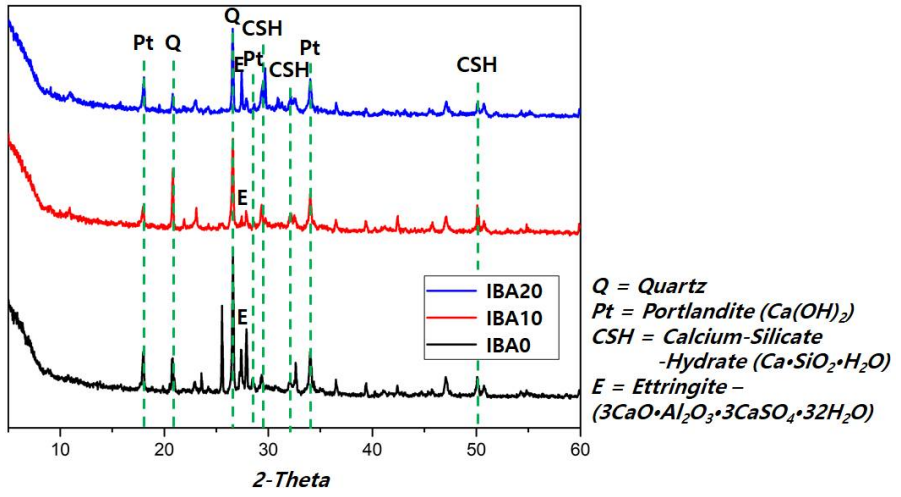

(**b**) XRD results after 7 days of curing ages

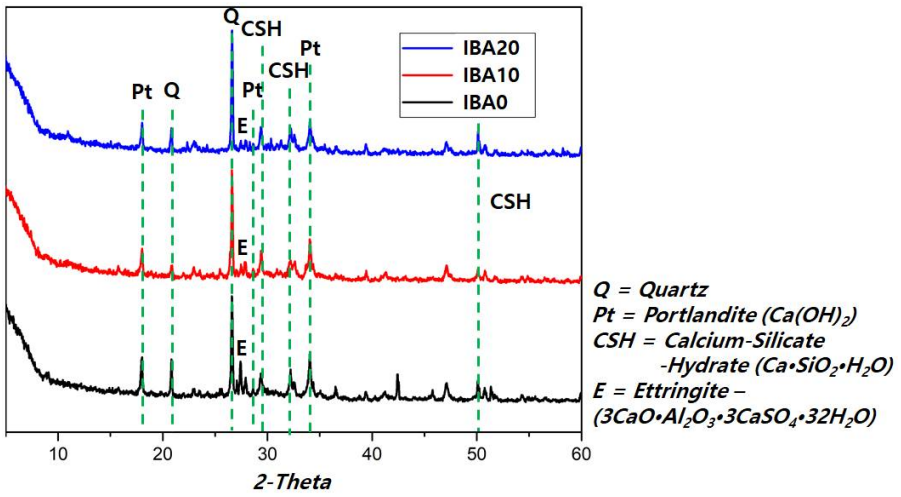

Figure 11. XRD results.

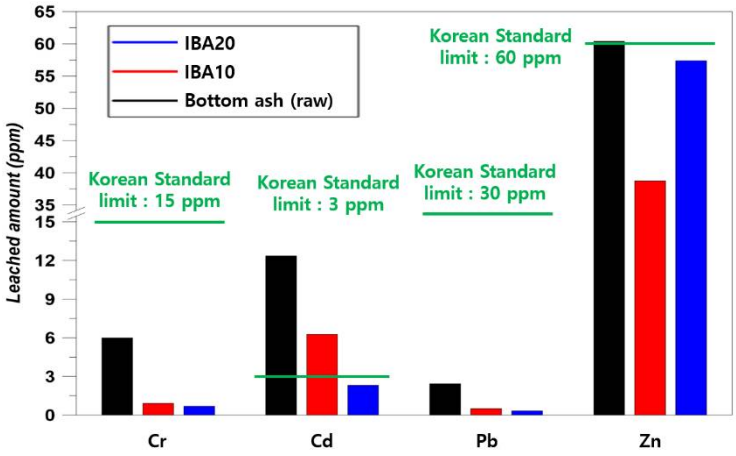

Figure 12. ICP-MS results.

The important point of leaching heavy metals is the limit. Although the standard for the limit of leaching the heavy metals would differ from country to country, this study analyzed the results using the Korean standard [36]. Korean construction materials limit Cr to 15 ppm, Cd to 3 ppm, Pb to 30 ppm, and Zn to 60 ppm. IBA10 showed enough margin with the leaching limit except for in the Cd figures. However, the leached amount of Cd from IBA10 may be acceptable. This is because IBA20 tends to meet Korean standards not only in the leaching of Cd but also in the leaching of all heavy metals, which can be sufficiently raised and lowered by the part of sampling and the amorphity of cement composites.

IBA20 also includes results that IBA could be used as up to 20% of fine aggregate depending on the results of Figure 12. This is because the leached heavy metals from IBA appeared below the Korean standards [36]. However, the total ppm of heavy metals tends to increase as IBA usage increases. Hence, the leaching of heavy metals is expected to exceed the Korean standard if IBA is used in excess of 20% of substitution.

Comprehensively, considering all the sections in this study, our results indicate that IBA could be used as a fine aggregate up to 20% of substitution. However, there are a few problems applying IBA to cement composites. First, the elimination or reduction of ASR reactive components is needed. ASR would create a significant cracking problem, therefore Na_2O and K_2O should be eliminated or reduced [35]. Second, pre-treatment of IBA before its application to cement composites should be performed due to the heavy metal content. In this study, the washing work was a simple cleaning using flowing water. However, Figure 12 demonstrates its importance in order to use IBA as a fine aggregate. Pre-treatment is needed to further reduce heavy metals contained in IBA. Following this, IBA could be used as a fine aggregate (a kind of lightweight aggregate) in the construction field.

4. Conclusions

This study performed experiments for using IBA as a substitution of fine aggregate. From the results of this study, it was demonstrated that IBA could be used as a substitution material. This factor was demonstrated by the compressive strength, SEM-BSE, XRD, MIP, and TCLP tests. The comprehensive conclusions are as follows.

1. Compressive strength was increased in all cases. IBA10 showed the highest value and IBA20 showed a relatively decreased value compared to IBA10. IBA10 showed the filler effect well, and IBA20 also showed filler effect. However, the reason for the reduction of compressive strength compared to IBA10 is that IBA is a kind of lightweight aggregate.
2. MIP and SEM-BSE showed how the fine particles fill the pores. This was demonstrated using SEM-BSE, showed visually, and MIP, showed quantitatively. The fine pores

were decreased with the increase of IBA, and the images of SEM-BSE clearly show that IBA is a kind of lightweight aggregate.

3. XRD and TCLP results showed the application risk of IBA to cement composites. XRD results indicated the possibility of ASR. On the other hand, TCLP results showed the low value of heavy metals. However, it is considered that a pre-treatment for eliminating or reducing the heavy metals in raw IBA is needed.

Author Contributions: Conceptualization, B.-H.W. and H.-G.K.; Investigation, I.-K.J. and D.-H.Y.; Methodology, I.-K.J. and S.-S.K.; Data curation, B.-H.W. and D.-H.Y.; Validation, S.-S.K. and J.-B.L.; Supervision H.-G.K. and J.-B.L.; Writing-original draft preparation, B.-H.W. and I.-K.J.; Corresponding, H.-G.K. All authors have read and agreed to the published version of the manuscript.

Funding: This research received no external funding.

Institutional Review Board Statement: Not applicable.

Informed Consent Statement: Not applicable.

Data Availability Statement: Not applicable.

Acknowledgments: This work was supported by the Korea Institute of Energy Technology Evaluation and Planning (KETEP) and the Ministry of Trade, Industry & Energy (MOTIE) of the Republic of Korea (No. 20183010025510).

Conflicts of Interest: The authors declare no conflict of interest.

References

1. Jurič, B.; Hanžič, L.; Ilić, R.; Samec, N. Utilization of municipal solid waste bottom ash and recycled aggregate in concrete. *Waste Manag.* **2006**, *26*, 1436–1442. [CrossRef]
2. Xuan, D.; Zhan, B.; Poon, C.S. Assessment of mechanical properties of concrete incorporating carbonated recycled concrete aggregates. *Cem. Concr. Compos.* **2016**, *65*, 67–74. [CrossRef]
3. Zhang, L. Production of bricks from waste materials—A review. *Constr. Build. Mater.* **2013**, *47*, 643–655. [CrossRef]
4. Quina, M.J.; Bordado, J.M.; Quinta-Ferreira, R.M. Recycling of air pollution control residues from municipal solid waste incineration into lightweight aggregates. *Waste Manag.* **2014**, *34*, 430–438. [CrossRef] [PubMed]
5. Pérez-Martínez, S.; Giro-Paloma, J.; Maldonado-Alameda, A.; Formosa, J.; Queralt, I.; Chimenos, J.M. Characterisation and partition of valuable metals from WEEE in weathered municipal solid waste incineration bottom ash, with a view to recovering. *J. Clean. Prod.* **2019**, *218*, 61–68. [CrossRef]
6. Loginova, E.; Volkov, D.; Van de Wouw, P.; Florea, M.; Brouwers, H. Detailed characterization of particle size fractions of municipal solid waste incineration bottom ash. *J. Clean. Prod.* **2019**, *207*, 866–874. [CrossRef]
7. Cabrera, M.; Galvin, A.P.; Agrela, F.; Beltran, M.G.; Ayuso, J. Reduction of leaching impacts by applying biomass bottom ash and recycled mixed aggregates in structural layers of roads. *Materials* **2016**, *9*, 228. [CrossRef]
8. Xu, F.; Wang, B.; Yang, D.; Qiao, Y.; Tian, Y. The steam gasification reactivity and kinetics of municipal solid waste chars derived from rapid pyrolysis. *Waste Manag.* **2018**, *80*, 64–72. [CrossRef] [PubMed]
9. Seo, Y. *Current MSW Management and Waste-to-Energy Status in the Republic of Korea*; Columbia University: New York, NY, USA, 2013; pp. 49–58.
10. Wiles, C.C. Municipal solid waste combustion ash: State-of-the-knowledge. *J. Hazard. Mater.* **1996**, *47*, 325–344. [CrossRef]
11. Zhu, W.; Chen, X.; Struble, L.J.; Yang, E.-H. Characterization of calcium-containing phases in alkali-activated municipal solid waste incineration bottom ash binder through chemical extraction and deconvoluted Fourier transform infrared spectra. *J. Clean. Prod.* **2018**, *192*, 782–789. [CrossRef]
12. Ge, D.; You, Z.; Chen, S.; Liu, C.; Gao, J.; Lv, S. The performance of asphalt binder with trichloroethylene: Improving the efficiency of using reclaimed asphalt pavement. *J. Clean. Prod.* **2019**, *232*, 205–212. [CrossRef]
13. Ghouleh, Z.; Shao, Y. Turning municipal solid waste incineration into a cleaner cement production. *J. Clean. Prod.* **2018**, *195*, 268–279. [CrossRef]
14. Le, N.H.; Razakamanantsoa, A.; Nguyen, M.-L.; Dao, P.-L.; Nguyen, D.H. Evaluation of physicochemical and hydromechanical properties of MSWI bottom ash for road construction. *Waste Manag.* **2018**, *80*, 168–174. [CrossRef]
15. Tang, P.; Florea, M.; Brouwers, H. Employing cold bonded pelletization to produce lightweight aggregates from incineration fine bottom ash. *J. Clean. Prod.* **2017**, *165*, 1371–1384. [CrossRef]
16. Lynn, C.J.; OBE, R.K.D.; Ghataora, G.S. Municipal incinerated bottom ash characteristics and potential for use as aggregate in concrete. *Constr. Build. Mater.* **2016**, *127*, 504–517. [CrossRef]
17. Siddique, R. Use of municipal solid waste ash in concrete. *Resour. Conserv. Recycl.* **2010**, *55*, 83–91. [CrossRef]

18. ASTM. C150, Standard specification for portland cement. In *Annual Book of ASTM Standards*; ASTM International: West Conshohocken, PA, USA, 2012.
19. ASTM. C33, standard specifications for concrete aggregates. In *ASTM Standard Book*; ASTM International: West Conshohocken, PA, USA, 2003.
20. Saffarzadeh, A.; Shimaoka, T.; Wei, Y.; Gardner, K.H.; Musselman, C.N. Impacts of natural weathering on the transformation/neoformation processes in landfilled MSWI bottom ash: A geoenvironmental perspective. *Waste Manag.* **2011**, *31*, 2440–2454. [CrossRef] [PubMed]
21. Meima, J.A.; Comans, R.N. The leaching of trace elements from municipal solid waste incinerator bottom ash at different stages of weathering. *Appl. Geochem.* **1999**, *14*, 159–171. [CrossRef]
22. Chimenos, J.; Fernández, A.; Miralles, L.; Segarra, M.; Espiell, F. Short-term natural weathering of MSWI bottom ash as a function of particle size. *Waste Manag.* **2003**, *23*, 887–895. [CrossRef]
23. ASTM. C109/109M, Standard test method for compressive strength of hydraulic cement mortars (using 2-in. or [50-mm] cube specimens). In *Annual Book of ASTM Standards*; ASTM International: West Conshohocken, PA, USA, 2016; Volume 4.
24. Gallé, C.J.C. Effect of drying on cement-based materials pore structure as identified by mercury intrusion porosimetry: A comparative study between oven-, vacuum-, and freeze-drying. *Cem. Concr. Res.* **2001**, *31*, 1467–1477. [CrossRef]
25. Diamond, S. Mercury porosimetry: An inappropriate method for the measurement of pore size distributions in cement-based materials. *Cem. Concr. Res.* **2000**, *30*, 1517–1525. [CrossRef]
26. Walker, H.N.; Lane, D.S.; Stutzman, P.E. *Petrographic Methods of Examining Hardened Concrete: A Petrographic Manual*; Federal Highway Administration: McLean, VA, USA, 2006.
27. USEPA. *Method 1311: Toxicity Characteristic Leaching Procedure (TCLP), Test Methods for Evaluating Solid Wast, Physical/Chemical Methods*; USEPA: Washington, DC, USA, 1992.
28. Mohammadhosseini, H.; Lim, N.H.A.S.; Tahir, M.M.; Alyousef, R.; Alabduljabbar, H.; Samadi, M. Enhanced performance of green mortar comprising high volume of ceramic waste in aggressive environments. *Constr. Build. Mater.* **2019**, *212*, 607–617. [CrossRef]
29. Jeon, I.K.; Qudoos, A.; Jakhrani, S.H.; Kim, H.G.; Ryou, J.-S. Investigation of sulfuric acid attack upon cement mortars containing silicon carbide powder. *Powder Technol.* **2020**, *359*, 181–189. [CrossRef]
30. Yu, A.-B.; Bridgwater, J.; Burbidge, A. On the modelling of the packing of fine particles. *Powder Technol.* **1997**, *92*, 185–194. [CrossRef]
31. Giro-Paloma, J.; Ribas-Manero, V.; Maldonado-Alameda, A.; Formosa, J.; Chimenos, J. Use of municipal solid waste incineration bottom ash and crop by-product for producing lightweight aggregate. In Proceedings of the 3rd International Conference on Innovative Materials, Structures and Technologies (IMST 2017), Riga, Latvia, 27–29 September 2017; p. 012126.
32. Karthika, R.; Vidyapriya, V.; Sri, K.N.; Beaula, K.M.G.; Harini, R.; Sriram, M. Experimental study on lightweight concrete using pumice aggregate. *Mater. Today Proc.* **2021**, *43*, 1606–1613. [CrossRef]
33. Zou, D.; Wang, Z.; Shen, M.; Liu, T.; Zhou, A. Improvement in freeze-thaw durability of recycled aggregate permeable concrete with silane modification. *Constr. Build. Mater.* **2021**, *268*, 121097. [CrossRef]
34. Huang, Q.; Qian, Z.; Hu, J.; Zheng, D.; Chen, L.; Zhang, M.; Yu, J. Investigation on the properties of aggregate-mastic interfacial transition zones (ITZs) in asphalt mixture containing recycled concrete aggregate. *Constr. Build. Mater.* **2021**, *269*, 121257. [CrossRef]
35. Jun, S.-S.; Jin, C.-S. Effect of Fineness Modulus of Reactive Aggregate on Alkali Silica Reaction. *Int. J. Concr. Struct. Mater.* **2010**, *4*, 119–125.
36. Yun, J.M.; Kim, T.H.; Song, Y.S. Analysis of leaching characteristics of heavy metals in bottom ash. *J. Korean Soc. Geosyst. Eng.* **2006**, *43*, 633–640.